Effects of Arctic stratospheric ozone changes on spring precipitation in the northwestern United States

Xuan Ma[1], Fei Xie[1*], Jianping Li[1,2], Xinlong Zheng[1], Wenshou Tian[3], Ruiqiang Ding[4], Cheng Sun[1], and Jiankai Zhang[3]

[1]*College of Global Change and Earth System Science, Beijing Normal University, Beijing, China*

[2]*Laboratory for Regional Oceanography and Numerical Modeling, Qingdao National Laboratory for Marine Science and Technology, Qingdao, China*

[3]*College of Atmospheric Sciences, Lanzhou University, Lanzhou, China*

[4]*State Key Laboratory of Numerical Modeling for Atmospheric Sciences and Geophysical Fluid Dynamics, Institute of Atmospheric Physics, Chinese Academy of Sciences, Beijing, China*

Submitted as an Article to: ***Atmospheric Chemistry and Physics***

4 December 2018

* Corresponding author:
Dr. Fei Xie, Email: xiefei@bnu.edu.cn.

Abstract

Using observations and reanalysis, we find that changes in April precipitation variations in the northwestern US are strongly linked to March Arctic stratospheric ozone (ASO). An increase in ASO can result in enhanced westerlies in the high and low latitudes of the North Pacific but weakened westerlies in the mid-latitudes. The anomalous circulation over the North Pacific can extend eastward to western North America, decreasing the water vapor concentration in the air over the northwestern United States and enhancing downwelling in the northwestern US, which results in decreased precipitation there, and vice versa for the decrease in ASO. Model simulations using WACCM4 support the statistical analysis of observations and reanalysis data, and further reveal that the ASO influences circulation anomalies over the northwestern US in two ways. Stratospheric circulation anomalies caused by the ASO changes can propagate downward to the troposphere in the North Pacific and then eastward to influence the strength of the circulation anomalies over the northwestern US. In addition, sea surface temperature anomalies over the North Pacific, which may be related to the ASO changes, would cooperate with the ASO changes to modify the circulation anomalies over the northwestern US. Our results suggest that ASO variations could be a useful predictor of spring precipitation changes in the northwestern US.

1. Introduction

Stratospheric circulation anomalies can affect tropospheric climate via chemical–radiative–dynamical feedback processes (Baldwin and Dunkerton, 2001; Graf and Walter, 2005; Cagnazzo and Manzini, 2009; Ineson and Scaife, 2009; Thompson et al., 2011; Reichler et al., 2012; Karpechko et al., 2014; Kidston et al., 2015; Li et al., 2016; Zhang et al., 2016; Wang et al., 2017). Since stratospheric ozone can influence stratospheric temperature and circulation via the atmospheric radiation balance (Tung, 1986; Haigh, 1994; Ramaswamy et al., 1996; Forster and Shine, 1997; Pawson and Naujokat, 1999; Solomon, 1999; Randel and Wu, 1999, 2007; Labitzke and Naujokat, 2000; Gabriel et al. 2007; Gillett et al. 2009; McCormack et al. 2011), the impact of ozone on tropospheric climate change has recently received widespread attention (e.g., Nowack et al. 2015, 2017, 2018).

In recent decades, Antarctic stratospheric ozone has decreased dramatically due to the increase in anthropogenic emissions of ozone depleting substances (Solomon, 1990, 1999; Ravishankara et al., 1994, 2009). Numerous studies have found that the decreased Antarctic ozone has contributed substantially to climate change in the Southern Hemisphere. The Southern Hemisphere circulation underwent a marked change during the late 20th century, with a slight poleward shift of the westerly jet (Thompson and Solomon, 2002; Archer and Caldeira, 2008). The poleward circulation shift would cause surface temperature anomalies by affecting localized wind patterns and associated thermal advection (Son et al., 2010; Thompson et al. 2011; Feldstein, 2011). Subsequent studies concluded that Antarctic ozone depletion is responsible for at least 50% of the circulation shift (Lu et al., 2009; Son et al., 2010; McLandress et al., 2011; Polvani et al., 2011; Hu et al., 2013; Gerber and Son, 2014; Waugh et al., 2015). In addition, the poleward displacement of the westerly jet has

been linked to an extension of the Hadley cell (Son et al., 2009, 2010; Min and Son, 2013) and variations in mid- to high-latitude precipitation during austral summer; i.e., increased rainfall in the subtropics and high latitudes and reduced rainfall in the mid-latitudes of the Southern Hemisphere (Son et al., 2009; Feldstein, 2011; Kang et al., 2011; Polvani et al., 2011). The changes in Antarctic ozone are not only related to the displacement of the westerly jet in the Southern Hemisphere, but also affect its intensity. Thompson and Solomon (2002) argued that Antarctic ozone depletion can also enhance westerly winds via the strong radiative cooling effect and thermal wind relationship. The westerly winds are enhanced from the stratosphere to the mid-latitude troposphere in the case of wave–mean flow interaction (Son et al., 2010; Thompson et al., 2011), thereby accelerating circumpolar currents in the mid-latitudes. Moreover, changes in subtropical drought, storm tracks and ocean circulation in the Southern Hemisphere are also closely related to Antarctic ozone variations (Yin, 2005; Russell et al., 2006; Son et al., 2009; Polvani et al., 2011; Bitz and Polvani, 2012).

The variations in Arctic stratospheric ozone (ASO) in the past five decades are quite different from those of Antarctic stratospheric ozone, as the multi-decadal loss of ASO is much smaller than that of Antarctic stratospheric ozone (WMO, 2011). However, sudden stratospheric warming in the Arctic (Randel, 1988; Charlton and Polvani, 2007; Manney et al., 2011; Manney and Lawrence, 2016) means that the year-to-year variability in ASO has an amplitude equal to or even larger than that of Antarctic stratospheric ozone. Thus, the effect of ASO on Northern Hemisphere climate change has also become a matter of concern.

Similar to the effects of winter stratospheric dynamical processes on the tropospheric North Atlantic Oscillation and the incidence of extreme weather events

(Baldwin and Dunkerton, 2001; Black et al., 2005, 2006, 2009), the depletion of spring ASO can cause circulation anomalies that influence the tropospheric North Atlantic and North Pacific sectors. Cheung et al. (2014) used the UK Met Office operational weather forecasting system and Karpechko et al. (2014) used ECHAM5 simulations to investigate the relationship between extreme Arctic ozone anomalies in 2011 and tropospheric climate. Smith and Polvani (2014) used an atmospheric global climate model to reveal a significant influence of ASO changes on tropospheric circulation, surface temperature, and precipitation when the amplitudes of the forcing ASO anomaly in the model are larger than those historically observed. Subsequently, using a fully coupled chemistry–climate model, Calvo et al. (2015) again confirmed that changes in ASO can produce robust anomalies in Northern Hemisphere temperature, wind, and precipitation. Furthermore, the effects of ASO on the Northern Hemisphere climate can be seen in observations. Ivy et al. (2017) presented observational evidence for the relationship between ASO and tropospheric climate, revealing that the maximum daily surface temperature anomalies in spring (March–April) in some regions of the Northern Hemisphere occurred during years with low ASO in March. Xie et al. (2016, 2017a, 2017b) demonstrated that the tropical climate can also be affected by ASO. They pointed out that stratospheric circulation anomalies caused by March ASO changes can rapidly extend to the lower troposphere and then propagate horizontally to the North Pacific in about 1 month, influencing the North Pacific sea surface temperature (SST) in April. The induced SST anomalies (Victoria Mode) associated with the circulation anomalies can influence El Niño–Southern Oscillation (ENSO) and tropical rainfall over a timescale of ~20 months.

As shown above, a large number of observations and simulations have shown that ASO variations have a significant impact on Northern Hemisphere tropospheric

94 climate, but few studies have focused on regional characteristics. Xie et al. (2018)
95 found that the ASO variations could significantly influence rainfall in the central
96 China, since the circulation anomalies over the North Pacific caused by ASO
97 variations can extend westward to China. This motivates us to investigate whether the
98 circulation anomalies extend eastward to affect the precipitation in North America. In
99 this study, we find a strong link between ASO and precipitation in the northwestern
100 US in spring. We focus on analyzing the characteristics of the impact of ASO on
101 precipitation in the northwestern US in spring and the associated mechanisms. The
102 remainder of this manuscript is organized as follows. Section 2 describes the data and
103 numerical simulations, and section 3 discusses the relationship between the ASO
104 anomalies and precipitation variations in the northwestern US, as well as the
105 underlying mechanisms. The results of simulations are presented in section 4, and
106 conclusions are given in section 5.

107 **2. Data and simulations**

108 The ASO variations is defined as the Arctic stratospheric ozone averaged over the
109 latitude of 60°–90°N at an altitude of 100–50 hPa after removing the seasonal cycle
110 and trend. Ozone values used in the present analysis are derived from the
111 Stratospheric Water and OzOne Satellite Homogenized (SWOOSH) dataset (Davis et
112 al., 2016), which is a collection of stratospheric ozone and water vapor measurements
113 obtained by multiple limb sounding and solar occultation satellites over the previous
114 30 years. Monthly mean ozone data from SWOOSH (1984–2016) is zonal–mean
115 gridded dataset at a horizontal resolution of 2.5° (latitude: 89°S to 89°N) and vertical
116 pressure range of 31 levels from 316 hPa to 1 hPa. Another set of ozone data is taken
117 from Global Ozone Chemistry and Related trace gas Data Records for the
118 Stratosphere (GOZCARDS, 1984–2013) project (Froidevaux et al., 2015) based on

high quality data from past missions (e.g., SAGE, HALOE data) and ongoing missions (ACE-FTS and Aura MLS). It is also a zonal–mean dataset with a meridional resolution of 10°, extending from the surface to 0.1 hPa (25 levels).

In addition, two sets of global precipitation reanalysis datasets are employed in this study: monthly mean precipitation data constructed by the Global Precipitation Climatology Project (GPCP), which is established by the World Climate Research program (WCRP) in 1986 aiming to observe and estimate the spatial and temporal global precipitation (Huffman et al., 1997), with a resolution of 2.5° latitude/longitude grid for the analysis period 1984–2016; global terrestrial rainfall dataset derived from the Global Precipitation Climatology Centre (GPCC) based on quality-controlled data from 67200 stations world-wide, with a resolution of 1.0° latitude/longitude grid. In addition, SST is taken from the UK Met Office Hadley Centre for Climate Prediction and Research SST (HadSST, Rayner et al., 2003). Other atmospheric datasets including monthly-mean wind and vertical velocity fields for the period 1984–2016 are obtained from the NCEP/Department of Energy (DOE) Reanalysis 2 (NCEP-2), regarded as an updated NCEP/NCAR Reanalysis Project (NCEP-1).

We use the Whole Atmosphere Community Climate Model version 4 (WACCM4), a part of the National Center for Atmospheric Research's Community Earth System Model (CESM), version 1.0.6, to investigate precipitation response in the northwestern United States to the ASO anomalies. WACCM4 encompasses the Community Atmospheric Model version 4 (CAM4) and as such includes all of its physical parameterizations (Neale et al., 2013). It uses a system made up of four components, namely atmosphere, ocean (specified SST), land, and sea ice (Holland et al., 2012) and has detailed middle–atmosphere chemistry. This improved version of

WACCM uses a finite-volume dynamical core, and it extends from the surface to approximately 145 km geometric altitude (66 levels), with a vertical resolution of about 1 km in the tropical tropopause layer and the lower stratosphere. Note that the simulations in the present paper are disable interactive chemistry as WACCM4-GHG scheme (Garcia et al., 2007) with a 1.9° × 2.5° horizontal resolution. WACCM4-GHG: The chemistry is specified in this scheme, i.e., the volume mixing ratios of forcings of O3, CO2, CH4, N2O, CFC11, CFC12 and so on are prescribed. More information can be seen in Marsh et al. (2013). The model's radiation scheme uses these conditions: fixed greenhouse gas (GHG) values (averages of emissions scenario A2 of the Intergovernmental Panel on Climate Change (WMO, 2003) over the period 1995–2005). The prescribed ozone forcing used in the experiments is a 12–month seasonal cycle averaged over the period 1995–2005 from CMIP5 ensemble mean ozone output. The Quasi Biennial Oscillation (QBO) phase signals with a 28–month fixed cycle are included in WACCM4 as an external forcing for zonal wind.

Seven time–slice experiments (R1–R7) and a transient experiment with specified ozone (R8) are designed to investigate the precipitation changes in the northwestern US due to the ASO anomalies. Details of the eight experiments are given in Table 1. Seven time–slice experiments (R1–R7) are run for 33 years, with the first 3 years excluded for the model spin–up and only the last 30 years are used. The transient experiment (R8) is run for 51 years.

3. Response of precipitation in the northwestern US to ASO anomalies in spring

Since the variations in ASO are most obvious in March due to the Arctic polar vortex break down (Manney et al., 2011), previous studies have reported that the ASO

changes in March have the strongest influence on the Northern Hemisphere (Ivy et al., 2017; Xie et al., 2017a). In addition, these studies pointed out that the changes in ASO affect the tropospheric climate with a lead of about 1–2 months, which is similar to the troposphere response to the Northern Hemisphere sudden stratospheric warmings (Baldwin and Dunkerton 2001; Black et al., 2005, 2006, 2009) and Southern Hemisphere stratospheric ozone depletion (Thompson and Solomon 2002); the relevant mechanisms have been investigated in detail by Xie et al. (2017a). We therefore show in Fig. 1 the correlation coefficients between ASO variations in March from SWOOSH and GOZCARDS data, and precipitation anomalies in April from GPCC and GPCP data over western North America. In all cases in Fig. 1 the March ASO changes are significantly anti-correlated with April precipitation anomalies in the northwestern US (mainly in Washington and Oregon), implying that positive spring ASO anomalies are associated with less spring precipitation in the northwestern US, and vice versa for the negative spring ASO anomalies. Note that since this kind of feature appears in the northwestern US, Fig. 1 shows only the west side of North America.

The correlation coefficients between March ASO variations and precipitation anomalies (January to December are in the same year) in the northwestern US are shown in Fig. 2. The correlation coefficients between March ASO variations and April precipitation anomalies in the northwestern US are the largest and are significant at the 95% confidence level. Note that the correlation coefficients between March ASO variations and July precipitation anomalies are also significant. The impact of March ASO on precipitation in the northwestern US in summer and the associated mechanisms are different from those considered in this study (not shown) and will be presented in another paper, but will not be investigated further here. March ASO

192 changes are not significantly correlated with simultaneous (March) precipitation
193 variations (Fig. 2), illustrating that the ASO changes lead precipitation anomalies by
194 about 1 month. Since the results from four sets of observations show a common
195 feature, and SWOOSH and GPCP data span a longer period, only SWOOSH ozone
196 and GPCP precipitation are used in the following analysis.

197 The above statistical analysis shows a strong negative correlation between March
198 ASO variations and April precipitation anomalies in the northwestern US, meaning
199 that the ASO can be used to predict changes in spring precipitation in the
200 northwestern US. The process and underlying mechanism that are responsible for the
201 impact of ASO anomalies on precipitation changes need further analysis.

202 Figure 3 shows the correlation coefficients between March ASO anomalies and
203 April zonal wind variations at 200, 500, and 850 hPa, respectively. The spatial
204 distribution of significant correlation coefficients over the North Pacific exhibits a
205 tripolar mode with a zonal distribution at 200 and 500 hPa; i.e. a positive correlation
206 in the high and low latitudes in the North Pacific and a negative correlation in
207 mid-latitudes. This implies that the increase in ASO can result in enhanced westerlies
208 in the high and low latitudes of the North Pacific but weakened westerlies in the
209 mid-latitudes, corresponding to the weakened Aleutian Low in April, and vice versa
210 for the decrease in ASO. The Aleutian Low acts as a bridge connecting variations in
211 ASO and circulation anomalies over the North Pacific (Xie et al., 2017a). At 850 hPa,
212 the anomalous circulation signal in the low latitudes of the North Pacific has
213 weakened and disappeared. It is evident that the anomalous changes in the zonal wind
214 over the North Pacific can extend westward to East Asia. Xie et al. (2018) identified
215 the effect of spring ASO changes on spring precipitation in China. Note that the

weakened westerlies in the mid-latitudes and the enhanced westerlies at low latitudes can also extend eastward to the western United States. This kind of circulation anomaly corresponds to two barotropic structures; i.e., an anomalous anticyclone in the Northeast Pacific and a cyclone in the southwestern United States at 500 hPa and 200 hPa. Coincidentally, the northwestern United States is located to the north of the intersection of the anticyclone and cyclone, corresponding to convergence of the airflow at high levels, which may lead to downwelling in the northwestern United States, and vice versa for negative March ASO anomalies.

To further validate our inference regarding the response of the circulation in the western United States to ASO changes, we analyze the differences between April horizontal wind anomalies during positive and negative March ASO anomaly events at 200, 500, and 850 hPa (Fig. 4). As in the increased ASO case, the difference shows an anomalous anticyclone in the Northeast Pacific and an anomalous cyclone in the southwestern United States. The climatological wind over the northwestern United States blows from west to east, bringing moisture from the Pacific to the western United States. Such circulation anomalies force an anomalous cyclone in the western United States in the middle and upper troposphere, which reduces the climatological wind. It would decrease the water vapor concentration in the air over the northwestern United States. In addition, the northwestern United States is located to the north of the intersection of the anticyclone and cyclone, suggesting downwelling flow in the region.

Figure 5a shows a longitude–latitude cross-section of differences in April vertical velocity anomalies averaged over 1000–500 hPa between positive and negative March ASO anomaly events. When the March ASO increases, anomalous downwelling is

found in the northwestern United States (115°–130° W). This situation may inhibit precipitation in the northwestern United States in April. Figure 5b depicts the longitude–height cross-section of differences in April vertical velocity averaged over 43°–50°N between positive and negative March ASO anomaly events, which further shows an anomalous downwelling over the northwestern United States when the ASO increases. Based on the above analysis, the circulation anomalies in the northwestern United States associated with positive March ASO anomalies may inhibit the formation of local precipitation in April, and vice versa for that with negative March ASO anomalies.

4. Simulations of the effect of ASO variations on precipitation in the northwestern US during spring

Using observations and reanalysis data, we investigated the relationship between March ASO and April precipitation in the northwestern US and revealed the underlying mechanisms in section 3. In this section, we use WACCM4 simulations (see section 2) to confirm the above conclusions. First, we check the model performance in simulating precipitation over western North America. Figure 6 shows the April precipitation climatology over the region 95°–140°W, 30°–63°N from the control experiment R1 (Table 1) and from GPCP for the period 1995–2005. The model simulates a center of high precipitation over the west coast of North America (Fig. 6a). It is clear that the spatial distribution of the simulated precipitation climatology is similar to that calculated by GPCP (Fig. 6b).

Figure 7a displays the differences in April precipitation between experiments R3 and R2. The pattern of simulated April precipitation anomalies forced by ASO changes in western North America (Fig. 7a) is different from that observed (Fig. 1);

i.e., the increased March ASO forces an increase in precipitation in the northwestern United States. The differences in April zonal wind at 200, 500, and 850 hPa between experiments R3 and R2 are shown in Fig. 7b, c, and d, respectively. The simulated pattern of April zonal wind anomalies in western North America (Fig. 7b, c and d) shifted a little further to the north than in the observations (Fig. 3). Comparing the global pattern of simulated April zonal wind anomalies with the observations, it is surprising to find that the positions of simulated zonal wind anomalies over the Northeast Pacific and western North America are shifted northward. This results in the simulated precipitation anomalies over western North America also shifting northward, so that a decrease in precipitation on the west coast of Canada in April is found in Fig. 7a. This explains why we find the pattern of simulated April precipitation anomalies in the North America (Fig. 7a) is nearly opposite to that observed (Fig. 1). Figure 7 shows that the results of the model simulation in which we only change the ASO forcing do not reflect the real situation of April precipitation anomalies in the northwestern United States, with a shift in position compared with observations. This leads us to consider whether other factors interact with March ozone to influence April precipitation in the northwestern United States.

Previous studies have found that the North Pacific SST has a significant effect on precipitation in the United States (e.g., Namias, 1983; Ting and Wang, 1997; Wang and Ting, 2000; Barlow et al., 2001; Lau et al., 2002; Wang et al., 2014). Figure 8a shows the correlation coefficients between regional averaged (43°–50°N, 115°–130°W) precipitation anomalies and SST variations in April. Interestingly, the results show that the distribution of correlation coefficients over the North Pacific has a meridional tripole structure, which is referred to as the Victoria Mode SST anomaly pattern. Xie et al. (2017a) demonstrated that the ASO has a lagged impact on the sea

surface temperature in the North Pacific mid–high latitudes based on observation and simulation. They showed that stratospheric circulation anomalies caused by ASO changes can rapidly extend to the lower troposphere in the high latitudes of the Northern Hemisphere. The circulation anomalies in the high latitudes of the lower troposphere take about a month to propagate to the North Pacific mid-latitudes and then influence the North Pacific SST. Figure 8b shows the correlation coefficients between March ASO (multiplied by –1) and April SST variations. The pattern in Fig. 8b is in good agreement with that in Fig. 8a. It is further found that removing the Victoria Mode signal from the time series of precipitation in the northwestern United States reduces the correlation coefficient between March ASO anomalies and filtered April precipitation variations in the northwestern United States to –0.40 (the correlation coefficient is –0.55 for the original time series, see Fig. 2), but it remains significant. Figure 8 indicates that the ASO possibly influences precipitation anomalies in the northwestern United States in two ways. First, the stratospheric circulation anomalies caused by the ASO changes can propagate downward to the North Pacific troposphere and eastward to influence precipitation over northwestern United States. Second, the ASO changes generate SST anomalies over the North Pacific that act as a bridge for ASO to affect precipitation in the northwestern United States (Xie et al., 2017a). The SST anomalies caused by ASO change likely interact with the direct changes in atmospheric circulation driven by the ASO change to jointly influence precipitation in the northwestern United States. Experiments R2 and R3 do not include the effects of SST, which may explain why the results of the model simulation in which we only change the ASO forcing do not reflect the observed precipitation anomalies in the northwestern United States (Fig. 7).

Two sets of experiments (R4 and R5) that include the joint effects of ASO and

SST change (Fig. 9) are added. Details of the experiments are given in Table 1. Figure 10 shows the differences in April precipitation and zonal wind between experiments R5 and R4. It is clear that the simulated changes in precipitation in the northwestern United States (Fig. 10a) are in good agreement with the observed anomalies shown in Fig. 1; i.e., the increase in March ASO forces a decrease in April precipitation in the northwestern United States. In addition, the spatial distributions of simulated zonal wind anomalies (Fig. 10b–d) are consistent with the observations (Fig. 3). Overall, the simulated precipitation and circulation in R4 and R5 are no longer shifted northward and are closer to the observations.

To further emphasize the importance of the joint effects of ASO and ASO-related SST anomalies on precipitation in the northwestern United States, we investigate whether the spring Victoria Mode-like SST anomalies alone could force the observed precipitation anomalies in the northwestern United States. Two sets of experiments are performed here (R6 and R7), in which only April SST anomalies over the North Pacific have been changed (Fig. 9). Details of the experiments are given in Table 1. Figure 11 shows the differences in April precipitation and zonal wind between experiments R7 and R6. The simulated precipitation anomalies over the west coast of the United States (Fig. 11a) are much weaker, and the simulated circulation anomalies (Fig. 11b–d) are quite different from those in Fig. 3. This suggests that the ASO-related North Pacific SST anomalies alone cannot force the observed precipitation anomalies in the northwestern United States, but that the combined effect of ASO and ASO-related North Pacific SST anomalies is required (Fig. 10).

In order to further confirm the possibly influence of ASO on precipitation in the northwestern United States, a transient experiment (1955–2005) based on the

atmosphere-ocean coupled WACCM4 model is added to confirm whether the ASO by itself can cause the Victoria SST mode in the North Pacific and rainfall anomalies in the northwestern United States. Note that the ozone forcing in the experiment is specified which is derived from the CMIP5 ensemble mean ozone output. Please refer to R8 in Table 1 for a detailed description of the experiment. Figure 12 shows the correlation coefficients between the specified March ASO variations and simulated April 500 hPa U, SST, and precipitation anomalies for the period 1955–2005. The significant and leading effects of the specified ASO anomalies on 500 hPa U, the Victoria mode in the North Pacific, and rainfall anomalies in the northwestern United States are well captured (Fig. 12). As the ozone forcing in the experiment is specified, the relationships between ASO and U and SST and precipitation could only be caused by ASO influencing U, and then U influencing SST and precipitation; the ASO changes are completely independent of polar vortex. The leading relationship between ASO and precipitation in the northwestern United States can be found in observations, time-slice experiments (R1–7), and a transient experiment with specified ozone (R8). Thus, we have shown that the relationship between March ASO and April precipitation in the northwestern US in the observations and the underlying mechanisms can be verified by WACCM4.

5. Discussion and summary

Many observations and simulations have shown that ASO variations have a significant impact on Northern Hemisphere tropospheric climate, but few studies have focused on regional characteristics. Using observations, reanalysis datasets, and WACCM4, we have shown that the March ASO changes have a significant effect on April precipitation in the northwestern United States (mainly in Washington and Oregon) with a lead of 1–2 months. When the March ASO is anomalously high, April

363 precipitation decreases in the northwestern United States, and vice versa for low ASO.

364 During positive ASO events, the zonal wind changes over the North Pacific
365 exhibit a tripolar mode with a zonal distribution; i.e., enhanced westerlies in the high
366 and low latitudes of the North Pacific, and weakened westerlies in the mid-latitudes.
367 The anomalous wind can extend eastward to North America, causing anomalous
368 circulation in western North America. The climatological wind over the northwestern
369 United States blows from west to east, bringing moisture from the Pacific to western
370 United States. Such circulation anomalies force an anomalous cyclone in the western
371 United States in the middle and upper troposphere, which reduces the climatological
372 wind. It would decrease the water vapor concentration in the air over the northwestern
373 United States. At the same time, downwelling in the northwestern US is enhanced.
374 The two processes possibly decrease April precipitation in the northwestern US.
375 When the March ASO decreases, the effect is just the opposite.

376 The WACCM4 model is used to confirm the statistical results of observations
377 and the reanalysis data. The results of the model simulation in which we only change
378 the ASO forcing do not reflect the observed precipitation anomalies in the
379 northwestern United States in April; i.e., the pattern of simulated April precipitation
380 and circulation anomalies in the western North America shifted a little further to the
381 north than observed. It is found that SST anomalies over North Pacific caused by
382 ASO changes are likely to interact with ASO changes to jointly influence
383 precipitation in the northwestern United States. Thus, the ASO influences
384 precipitation anomalies over the northwestern United States in two ways. First, the
385 stratospheric circulation anomalies caused by the ASO change can propagate
386 downward to the North Pacific troposphere and directly influence precipitation over

387 the northwestern United States. Second, the ASO changes generate SST anomalies
388 over the North Pacific that act as a bridge (Xie et al., 2017a), allowing the ASO
389 changes to affect precipitation in the northwestern United States.

390 It is well known that the spring ASO variations are related to changes in the
391 winter Arctic stratospheric vortex (SPV). The strength of the winter SPV can affect
392 spring ASO, and then the ASO affects tropospheric teleconnection and precipitation
393 in the northwestern United States (indirect effect of SPV). The strength of the winter
394 SPV may also have a direct leading effect on tropospheric teleconnection (Baldwin
395 and Dunkerton, 2001; Black et al., 2005, 2006, 2009) and precipitation in the
396 northwestern United States in spring. A question arises here, whether the stratospheric
397 polar vortex variability in late winter can be a better factor for leading spring
398 precipitation variations in the northwestern United States than the spring ASO
399 anomalies? Figure 13 shows the correlation coefficients between the February SPV
400 (multiplied by –1) index and April 200 hPa zonal wind and precipitation variations
401 (Fig. 13a and b), and between March ASO and April 200 hPa zonal wind and
402 precipitation (Fig. 13c and d). The SPV index is defined as the strength of the
403 stratospheric polar vortex, following Zhang et al. (2018). It is found that the
404 relationship between the strength of February SPV and the variations in 200 hPa zonal
405 wind and precipitation is significant (Fig. 13a and b), indicating indirect or direct
406 effects of winter SPV on spring tropospheric climate. However, the relationship isn't
407 stronger than that between March ASO and April 200 hPa zonal wind and
408 precipitation (Fig. 13c and d). In this study, we try to state that the ASO changes

could influence precipitation in the northwestern United States, emphasizing the influence of stratospheric ozone on tropospheric regional climate. As for the effect of coupling between dynamical and radiative processes in spring on precipitation is an interesting question that deserves further investigation.

Acknowledgments. Funding for this project was provided by the National Natural Science Foundation of China (41630421, 41790474 and 41575039). We acknowledge ozone datasets from the SWOOSH and GOZCARDS; precipitation from GPCC and GPCP; Meteorological fields from NCEP2, SST from the UK Met Office Hadley Centre, and WACCM4 from NCAR.

418 **References:**

419 Archer, C. L. and Caldeira, K.: Historical trends in the jet streams, Geophys. Res.
420 Lett., 35, L08803, doi:10.1029/2008GL033614, 2008.

421 Baldwin, M. P. and Dunkerton, T. J.: Stratospheric harbingers of anomalous weather
422 regimes, Science, 294, 581–584, doi:10.1126/science.1063315, 2001.

423 Barlow, M., Nigam, S., and Berbery, E. H.: ENSO, Pacific decadal variability, and US
424 summertime precipitation, drought, and stream flow, J. Climate, 14, 2105–2128,
425 doi:10.1175/1520-0442(2001)014<2105:EPDVAU>2.0.CO;2, 2001.

426 Bitz, C. M. and Polvani, L. M.: Antarctic climate response to stratospheric ozone
427 depletion in a fine resolution ocean climate model, Geophys. Res. Lett., 39,
428 L20705, doi:10.1029/2012GL053393, 2012.

429 Black, R. X., Mcdaniel, B. A., and Robinson, W. A.: Stratosphere Troposphere
430 Coupling during Spring Onset, J. Climate, 19, 4891–4901,
431 doi:10.1175/Jcli3907.1, 2005.

432 Black, R. X., and Mcdaniel, B. A.: The Dynamics of Northern Hemisphere
433 Stratospheric Final Warming Events, J. Atmos. Sci., 64, 2932–2946,
434 doi:10.1175/Jas3981.1, 2006.

435 Black, R. X. and Mcdaniel, B. A.: SubMonthly polar vortex variability and
436 stratosphere-troposphere coupling in the Arctic, J. Climate, 22, 5886–5901,
437 doi:10.1175/2009JCLI2730.1, 2009.

438 Cagnazzo, C. and Manzini, E.: Impact of the Stratosphere on the Winter Tropospheric
439 Teleconnections between ENSO and the North Atlantic and European Region, J.

Climate, 22, 1223–1238, doi:10.1175/2008JCLI2549.1, 2009.

Calvo, N., Polvani, L. M., and Solomon, S.: On the surface impact of Arctic stratospheric ozone extremes, Environ. Res. Lett., 10, 094003, doi:10.1088/1748-9326/10/9/094003, 2015.

Charlton, A. J. and Polvani, L. M.: A new look at stratospheric sudden warmings. Part I: Climatology and modeling benchmarks, J. Climate, 20, 449–469, doi:10.1175/JCLI3996.1, 2007.

Cheung, J. C. H., Haigh, J. D., and Jackson, D. R.: Impact of EOS MLS ozone data on medium-extended range ensemble weather forecasts, J. Geophys. Res., 119, 9253–9266, doi:10.1002/2014JD021823, 2014.

Davis, S. M, Rosenlof, K. H., Hassler, B., Hurst, D. F., Read, W. G., Vomel, H., Selkirk, H., Fujiwara, M., and Damadeo, R.: The Stratospheric Water and Ozone Satellite Homogenized (SWOOSH) database: a long-term database for climate studies, Earth Syst Sci Data, 8, 461–490, doi:10.5194/essd-8-461-2016, 2016.

Feldstein, S. B.: Subtropical Rainfall and the Antarctic Ozone Hole, Science, 332, 925–926, doi:10.1126/science.1206834, 2011.

Forster, P. M. D. and Shine, K. P.: Radiative forcing and temperature trends from stratospheric ozone changes, J. Geophys. Res., 102, 10841–10855, doi:10.1029/96JD03510, 1997.

Froidevaux, L., Anderson, J., Wang, H.-J., Fuller, R. A., Schwartz, M. J., Santee, M. L., Livesey, N. J., Pumphrey, H. C., Bernath, P. F., Russell III, J. M., and

McCormick, M. P.: Global OZone Chemistry And Related trace gas Data records for the Stratosphere (GOZCARDS): methodology and sample results with a focus on HCl, H2O, and O-3, Atmos. Chem. Phys., 15, 10471–10507, doi:10.5194/acp-15-10471-2015, 2015.

Gabriel, A., Peters, D., Kirchner, I., and Graf, H. F.: Effect of zonally asymmetric ozone on stratospheric temperature and planetary wave propagation, Geophys. Res. Lett., 34, L06807, doi:10.1029/2006GL028998, 2007.

Garcia, R. R., Marsh, D. R., Kinnison, D. E., Boville, B. A., and Sassi, F.: Simulation of secular trends in the middle atmosphere, 1950–2003, J. Geophys. Res., 112, D09301, doi:10.1029/2006JD007485, 2007.

Gerber, E. P. and Son, S. W.: Quantifying the Summertime Response of the Austral Jet Stream and Hadley Cell to Stratospheric Ozone and Greenhouse Gases, J. Climate, 27, 5538–5559, doi:10.1175/JCLI-D-13-00539.1, 2014.

Gillett, N. P., Scinocca, J. F., Plummer, D. A., and Reader, M. C.: Sensitivity of climate to dynamically-consistent zonal asymmetries in ozone, Geophys. Res. Lett., 36, L10809, doi:10.1029/2009GL037246, 2009.

Graf, H. F. and Walter, K.: Polar vortex controls coupling of North Atlantic Ocean and atmosphere, Geophys. Res. Lett., 32, L01704, doi:10.1029/2004GL020664, 2005.

Haigh, J. D.: The Role of Stratospheric Ozone in Modulating the Solar Radiative Forcing of Climate, Nature, 370, 544–546, doi:10.1038/370544a0, 1994.

Holland, M. M., Bailey, D. A., Briegleb, B. P., Light, B., and Hunke, E.: Improved

484 Sea Ice Shortwave Radiation Physics in CCSM4: The Impact of Melt Ponds and
485 Aerosols on Arctic Sea Ice, J. Climate, 25, 1413–1430,
486 doi:10.1175/JCLI-D-11-00078.1, 2012.
487 Hu, Y., Tao, L., and Liu, J.: Poleward expansion of the Hadley circulation in CMIP5
488 simulations, Adv. Atmos. Sci., 30, 790–795, doi:10.1007/s00376-012-2187-4,
489 2013.
490 Huffman, G. J., Adler, R. F., Arkin, P., Chang, A., Ferraro, R., Gruber, A., Janowiak, J.,
491 McNab, A., Rudolf, B., and Schneider, U.: The Global Precipitation Climatology
492 Project (GPCP) Combined Precipitation Dataset, B. Am. Meteorol. Soc., 78, 5–
493 20, doi:10.1175/1520-0477(1997)078<0005:TGPCPG>2.0.Co;2, 1997.
494 Ineson, S. and Scaife, A. A.: The role of the stratosphere in the European climate
495 response to El Nino, Nat. Geosci., 2, 32–36, doi:10.1038/NGEO381, 2009.
496 Ivy, D. J., Solomon, S., Calvo, N., and Thompson, D. W.: Observed connections of
497 Arctic stratospheric ozone extremes to Northern Hemisphere surface climate,
498 Environ. Res. Lett., 12, 024004, doi:10.1088/1748-9326/aa57a4, 2017.
499 Kang, S. M., Polvani, L. M., Fyfe, J. C., and Sigmond, M.: Impact of Polar Ozone
500 Depletion on Subtropical Precipitation, Science, 332, 951–954,
501 doi:10.1126/science.1202131, 2011.
502 Karpechko, A. Y., Perlwitz, J., and Manzini, E.: A model study of tropospheric
503 impacts of the Arctic ozone depletion 2011, J. Geophys. Res., 119, 7999–8014,
504 doi:10.1002/2013JD021350, 2014.
505 Kidston, J., Scaife, A. A., Hardiman, S. C., Mitchell, D. M., Butchart, N., Baldwin, M.

506 P., and Gray, L. J.: Stratospheric influence on tropospheric jet streams, storm
507 tracks and surface weather, Nat. Geosci., 8, 433–440, doi:10.1038/NGEO2424,
508 2015.
509 Labitzke, K. and Naujokat, B.: The lower Arctic stratosphere in winter since 1952,
510 Sparc Newsletter, 15, 11–14, 2000.
511 Lau, K. M., Kim, K. M., and Shen, S. S.: Potential predictability of seasonal
512 precipitation over the U.S. from canonical ensemble correlation
513 predictions, Geophys. Res. Lett., 29, 1–4, doi:10.1029/2001GL014263, 2002.
514 Li, F., Vikhliaev, Y. V., Newman, P. A., Pawson, S., Perlwitz, J., Waugh, D. W., and
515 Douglass, A. R.: Impacts of Interactive Stratospheric Chemistry on Antarctic and
516 Southern Ocean Climate Change in the Goddard Earth Observing System,
517 Version 5 (GEOS-5), J. Climate, 29, 3199–3218, doi:10.1175/JCLI-D-15-0572.1,
518 2016.
519 Lu, J., Deser, C., and Reichler, T.: Cause of the widening of the tropical belt since
520 1958, Geophys. Res. Lett., 36, L03803, doi:10.1029/2008GL036076, 2009.
521 Manney, G. L., Santee, M. L., Rex, M., Livesey, N. J., Pitts, M. C., Veefkind, P., Nash,
522 E. R., Wohltmann, I., Lehmann, R., Froidevaux, L., Poole, L. R., Schoeberl, M.
523 R., Haffner, D. P., Davies, J., Dorokhov, V., Gernandt, H., Johnson, B., Kivi, R.,
524 Kyrö, E., Larsen, N., Levelt, P. F., Makshtas, A., McElroy, C. T., Nakajima, H.,
525 Parrondo, M. C., Tarasick, D. W., von der Gathen, P., Walker, K. A., and
526 Zinoviev, N. S.: Unprecedented Arctic ozone loss in 2011, Nature, 478, 469–475,
527 https://doi.org/10.1038/nature10556, 2011.

528 Manney, G. L. and Lawrence, Z. D.: The major stratospheric final warming in 2016:
529 dispersal of vortex air and termination of Arctic chemical ozone loss, Atmos.
530 Chem. Phys., 16, 15371–15396, doi:10.5194/acp-16-15371-2016, 2016.
531 Marsh, D. R., Mills, M. J., Kinnison, D. E., Lamarque, J. F., Calvo, N., and Polvani, L.
532 M.: Climate Change from 1850 to 2005 Simulated in CESM1(WACCM), J.
533 Climate, 26, 7372–7391, doi:10.1175/JCLI-D-12-00558.1, 2013.
534 McCormack, J. P., Nathan, T. R., and Cordero, E. C.: The effect of zonally
535 asymmetric ozone heating on the Northern Hemisphere winter polar stratosphere,
536 Geophys. Res. Lett., 38, 1–5, doi: 10.1029/2010GL045937, 2011.
537 McLandress, C., Shepherd, T. G., Scinocca, J. F., Plummer, D. A., Sigmond, M.,
538 Jonsson, A. I., and Reader, M. C.: Separating the dynamical effects of climate
539 change and ozone depletion. Part II: Southern Hemisphere troposphere, J.
540 Climate, 24, 1850–1868, doi:10.1175/2010JCLI3958.1, 2011.
541 Min, S. K. and Son, S. W.: Multimodel attribution of the Southern Hemisphere
542 Hadley cell widening: Major role of ozone depletion, J. Geophys. Res., 118,
543 3007–3015, doi:10.1002/jgrd.50232, 2013.
544 Namias, J.: Some causes of U.S. drought, J. Clim. Appl. Meteorol., 22, 30–39,
545 doi:10.1175/1520-0450(1983)022<0030:Scousd>2.0.Co;2, 1983.
546 Neale, R. B., Richter, J., Park, S., Lauritzen, P. H., Vavrus, S. J., Rasch, P. J., and
547 Zhang, M. H.: The Mean Climate of the Community Atmosphere Model (CAM4)
548 in Forced SST and Fully Coupled Experiments, J. Climate, 26, 5150–5168,
549 doi:10.1175/JCLI-D-12-00236.1, 2013.

Nowack, P. J., Abraham, N. L., Maycock, A. C., Braesicke, P., Gregory, J. M., Joshi, M. M., Osprey, A., and Pyle, J. A.: A large ozone-circulation feedback and its implications for global warming assessments, Nat. Clim. Change, 5, 41–45, doi:10.1038/NCLIMATE2451, 2015.

Nowack, P. J., Braesicke, P., Abraham, N. L., and Pyle, J. A.: On the role of ozone feedback in the ENSO amplitude response under global warming, Geophys. Res. Lett., 44, 3858–3866, doi: 10.1002/2016GL072418, 2017.

Nowack, P. J., Abraham, N. L., Braesicke, P., and Pyle, J. A.: The impact of stratospheric ozone feedbacks on climate sensitivity estimates, J. Geophys. Res., 123, 4630–4641, doi: 10.1002/2017JD027943, 2018.

Pawson, S. and Naujokat, B.: The cold winters of the middle 1990s in the northern lower stratosphere, J. Geophys. Res., 104, 14209–14222, doi:10.1029/1999JD900211, 1999.

Polvani, L. M., Waugh, D. W., Correa, G. J., and Son, S.-W.: Stratospheric ozone depletion: The main driver of twentieth-century atmospheric circulation changes in the Southern Hemisphere, J. Climate, 24, 795–812, doi:10.1175/2010JCLI3772.1, 2011.

Ramaswamy, V., Schwarzkopf, M. D., and Randel, W. J.: Fingerprint of ozone depletion in the spatial and temporal pattern of recent lower-stratospheric cooling, Nature, 382, 616–618, doi:10.1038/382616a0, 1996.

Randel, W. J.: The Seasonal Evolution of Planetary-Waves in the Southern-Hemisphere Stratosphere and Troposphere, Quarterly Journal of the

572 Royal Meteorological Society, 114, 1385–1409, doi:10.1002/qj.49711448403,
573 1988.
574 Randel, W. J. and Wu, F.: Cooling of the arctic and antarctic polar stratospheres due to
575 ozone depletion, J. Climate, 12, 1467–1479,
576 doi:10.1175/1520-0442(1999)012<1467:COTAAA>2.0.Co;2, 1999.
577 Randel, W. J. and Wu, F.: A stratospheric ozone profile data set for 1979-2005:
578 Variability, trends, and comparisons with column ozone data, J. Geophys. Res.,
579 112, D06313, doi:10.1029/2006JD007339, 2007.
580 Ravishankara, A. R., Turnipseed, A. A., Jensen, N. R., Barone, S., Mills, M., Howard,
581 C. J., and Solomon, S.: Do hydrofluorocarbons destroy stratospheric ozone?,
582 Science, 263, 71–75, doi:10.1126/science.263.5143.71, 1994.
583 Ravishankara, A. R., Daniel, J. S., and Portmann, R. W.: Nitrous oxide (N2O): the
584 dominant ozone-depleting substance emitted in the 21st century, Science, 326,
585 123–125, doi:10.1126/science.1176985, 2009.
586 Rayner, N. A., Parker, D. E., Horton, E. B., Folland, C. K., Alexander, L. V., and
587 Rowell, D. P.: Global analyses of sea surface temperature, sea ice, and night
588 marine air temperature since the late nineteenth century, J. Geophys. Res., 108,
589 4407, 2003.
590 Reichler, T., Kim, J., Manzini, E., and Kroger, J.: A stratospheric connection to
591 Atlantic climate variability, Nat. Geosci., 5, 783–787, doi:10.1038/NGEO1586,
592 2012.
593 Russell, J. L., Dixon, K. W., Gnanadesikan, A., Stouffer, R. J., and Toggweiler, J. R.:

The Southern Hemisphere westerlies in a warming world: Propping open the door to the deep ocean, J. Climate, 19, 6382–6390, doi:10.1175/JCLI3984.1, 2006.

Smith, K. L. and Polvani, L. M.: The surface impacts of Arctic stratospheric ozone anomalies, Environ. Res. Lett., 9, 074015, doi:10.1088/1748-9326/9/7/074015, 2014.

Solomon, S.: Antarctic ozone: Progress towards a quantitative understanding, Nature, 347, 354, doi:10.1038/347347a0, 1990.

Solomon, S.: Stratospheric ozone depletion: A review of concepts and history, Rev. Geophys., 37, 275–316, doi:10.1029/1999RG900008, 1999.

Son, S.-W., Tandon, N. F., Polvani, L. M., and Waugh, D. W.: Ozone hole and Southern Hemisphere climate change, Geophys. Res. Lett., 36, L15705, doi:10.1029/2009GL038671, 2009.

Son, S.-W., Gerber, E. P., Perlwitz, J., Polvani, L. M., Gillett, N. P., Seo, K.-H., Eyring, V., Shepherd, T. G., Waugh, D., Akiyoshi, H., Austin, J., Baumgaertner, A., Bekki, S., Braesicke, P., Brühl, C., Butchart, N., Chipperfield, M. P., Cugnet, D., Dameris, M., Dhomse, S., Frith, S., Garny, H., Garcia, R., Hardiman, S. C., Jöckel, P., Lamarque, J. F., Mancini, E., Marchand, M., Michou, M., Nakamura, T., Morgenstern, O., Pitari, G., Plummer, D. A., Pyle, J., Rozanov, E., Scinocca, J. F., Shibata, K., Smale, D., Teyssèdre, H., Tian, W., and Yamashita, Y.: Impact of stratospheric ozone on Southern Hemisphere circulation change: A multimodel assessment, J. Geophys. Res., 115, D00M07, doi.org/10.1029/2010JD014271,

2010.

Thompson, D. W. J. and Solomon, S.: Interpretation of recent Southern Hemisphere climate change, Science, 296, 895–899, doi:10.1126/science.1069270, 2002.

Thompson, D. W. J., Solomon, S., Kushner, P.‘J., England, M. H., Grise, K. M., and Karoly, D. J.: Signatures of the Antarctic ozone hole in Southern Hemisphere surface climate change, Nature Geosci., 4, 741–749, doi:10.1038/NGEO1296, 2011.

Ting, M. and Wang, H.: Summertime US Precipitation Variability and Its Relation toPacific Sea Surface Temperature, J. Climate, 10, 1853–1873, doi:10.1175/1520-0442(1997)010<1853:SUSPVA>2.0.CO;2, 1997.

Tung, K. K.: On the Relationship between the Thermal Structure of the Stratosphere and the Seasonal Distribution of Ozone, Geophys. Res. Lett., 13, 1308–1311, doi:10.1029/GL013i012p01308, 1986.

Wang, F., Yang, S., Higgins, W., Li, Q. P., and Zuo, Z. Y.: Long-term changes in total and extreme precipitation over China and the U.S. and their links to oceanic-atmospheric features, Int. J. Climatol., 34, 286–302, doi:10.1002/joc.3685, 2014.

Wang, H. and Ting, M. F.: Covariabilities of winter US precipitation and Pacific Sea surface temperatures, J. Climate, 13, 3711–3719, doi:10.1175/1520-0442(2000)013<3711:Cowusp>2.0.Co;2, 2000.

Wang, L., Ting, M., Kushner, P. J.: A robust empirical seasonal prediction of winter NAO and surface climate, Sci. Rep., 7, 279, 2017.

638 Waugh, D. W., Garfinkel, C. I., and Polvani, L. M.: Drivers of the Recent Tropical
639 Expansion in the Southern Hemisphere: Changing SSTs or Ozone Depletion?, J.
640 Climate, 28, 6581–6586, doi:10.1175/JCLI-D-15-0138.1, 2015.
641 WMO: Scientific Assessment of Ozone depletion: 2002. In: Global Ozone Research
642 and Monitoring Project, Report No. 47, Geneva, 498 pp., 2003.
643 WMO: Scientific Assessment of Ozone Depletion: 2010. WMO Tech. Note 52, World
644 Meteorological Organization, Geneva, Switzerland, 516 pp., 2011.
645 Xie, F., Li, J., Tian, W., Fu, Q., Jin, F.-F., Hu, Y., Zhang, J., Wang, W., Sun, C., Feng,
646 J., Yang, Y., and Ding, R.: A connection from Arctic stratospheric ozone to El
647 Niño-Southern Oscillation, Environ. Res. Lett., 11, 124026,
648 doi:10.1088/1748-9326/11/12/124026, 2016.
649 Xie, F., Li, J., Zhang, J., Tian, W., Hu, Y., Zhao, S., Sun, C., Ding, R., Feng, J., Yang,
650 Y.: Variations in North Pacific sea surface temperature caused by Arctic
651 stratospheric ozone anomalies, Environ. Res. Lett., 12, 114023,
652 doi:10.1088/1748-9326/aa9005, 2017a.
653 Xie, F., Zhang, J., Sang, W., Li, Y., Qi, Y., Sun, C., and Shu, J.: Delayed effect of
654 Arctic stratospheric ozone on tropical rainfall, Atmos. Sci. Lett., 18, 409–416,
655 2017b.
656 Xie, F., Ma, X., Li, J., Huang, J., Tian, W., Zhang, J., Hu, Y., Sun, C., Zhou, X., Feng,
657 J., Yang, Y.: An advanced impact of Arctic stratospheric ozone changes on spring
658 precipitation in China, Clim. Dyn., 51, 4029–4041,
659 do:10.1007/s00382-018-4402-1, 2018.

660 Yin, J. H.: A consistent poleward shift of the storm tracks in simulations of 21st
661 century climate, Geophys. Res. Lett., 32, L18701, doi:10.1029/2005GL023684,
662 2005.
663 Zhang, J. K., Tian, W. S., Chipperfield, M. P., Xie, F., and Huang, J. L.: Persistent
664 shift of the Arctic polar vortex towards the Eurasian continent in recent decades,
665 Nat. Clim. Change., 6, 1094–1099, doi:10.1038/nclimate3136, 2016.
666 Zhang J. K., Tian, W. S., Xie, F., Chipperfield, M. P., Feng, W. H., Son, S-W.,
667 Abraham, N. L., Archibald, A. T., Bekki, S., Butchart, N., Deushi, M., Dhomse,
668 S., Han, Y. Y., Jöckel, P., Kinnison, D., Kirner, O., Michou, M., Morgenstern, O.,
669 O'Connor, F. M., Pitari, G., Plummer, D. A., Revell, L. E., Rozanov, E., Visioni,
670 D., Wang, W. K., Zeng, G.: Stratospheric ozone loss over the Eurasian continent
671 induced by the polar vortex shift, Nat. Commun., 9, 206,
672 doi.org/10.1038/s41467-017-02565-2, 2018.

673 **Table 1**. CESM-WACCM4 experiments with various specified ozone and SST
674 forcing.

Exp[*1]	Specified ozone and SST forcing	Other forcing
R1	Time-slice run as the control experiment used case F_2000_WACCM_SC. The specified ozone forcing is a 12-month cycle of monthly ozone averaged from 1995 to 2005. The specified SST forcing is a 12-month cycle of monthly SST averaged from 1995 to 2005.	Fixed solar constant, fixed greenhouse gas (GHG) values (averages of emissions scenario A2 of the Intergovernmental Panel on Climate Change (WMO, 2003) over the period 1995–2005), volcanic aerosols (from the Stratospheric Processes and their Role in Climate (SPARC) Chemistry–Climate Model Validation (CCMVal) REF-B2 scenario recommendations), and QBO phase signals with a 28-month zonal wind fixed cycle.
R2	Same as R1, except that the March ozone in the region 30°–90°N at 300–30 hPa[*2] is decreased by 15% compared with R1.	Same as R1
R3	Same as R1, except that March ozone in the region 30°–90°N at 300–30 hPa is increased by 15% compared with R1.	Same as R1
R4	Same as R2, except that SST anomalies in the region 0°–70°N and 120°E–90°W related to negative ASO anomalies[*3] is added in the SST forcing in April.	Same as R1
R5	Same as R3, except that SST anomalies in the region 0°–70°N and 120°E–90°W related to positive ASO anomalies[*4] is added in the SST forcing in April.	Same as R1
R6	Same as R1, except that SST anomalies in the region 0°–70°N and 120°E–90°W related to negative ASO anomalies[*3] is added in the SST forcing in April.	Same as R1

R7	Same as R1, except that SST anomalies in the region 0°–70°N and 120°E–90°W related to positive ASO anomalies[*4] is added in the SST forcing in April.	Same as R1
R8	Transient run using case B_1955–2005_WACCM_SC_CN in CESM. E_1 is a historical simulation covering the period 1955–2005. Note that the specified ozone forcing for 1955–2005 was derived from the CMIP5 ensemble mean ozone output. The specified ozone forcing was named ghg_forcing_1955-2005_CMIP5_EnsMean.c140414.nc, and can be downloaded at https://svn-ccsm-inputdata.cgd.ucar.edu/trunk/inputdata/atm/waccm/ub/ghg_forcing_1955-2005_CMIP5_EnsMean.c140414.nc	All natural and anthropogenic external forcings for R8 based on observation and from original CESM input data.

[*1]Integration time for time-slice runs is 33 years and for transient run is 51 years.

[*2]To avoid the effect of the boundary of ozone change on the Arctic stratospheric circulation simulation, the replaced region (30°–90°N, 300–30 hPa) was larger than the region used to define the ASO index (60°–90°N, 100–50 hPa).

[*3]For SST anomalies, see Fig. 9a.

[*4]For SST anomalies, see Fig. 9b.

Table 2. Selected positive and negative years for March ASO anomaly events based on SWOOSH data for the period 1984–2016. Positive and negative March ASO anomaly events are defined using a normalized time series of March ASO variations from 1984 to 2016. Values larger than 1 standard deviation are defined as positive March ASO anomaly events, and those below –1 standard deviation are defined as negative March ASO anomaly events.

Positive March ASO anomaly events	Negative March ASO anomaly events
1998, 1999, 2001, 2004, 2010	1993, 1995, 1996, 2000, 2011

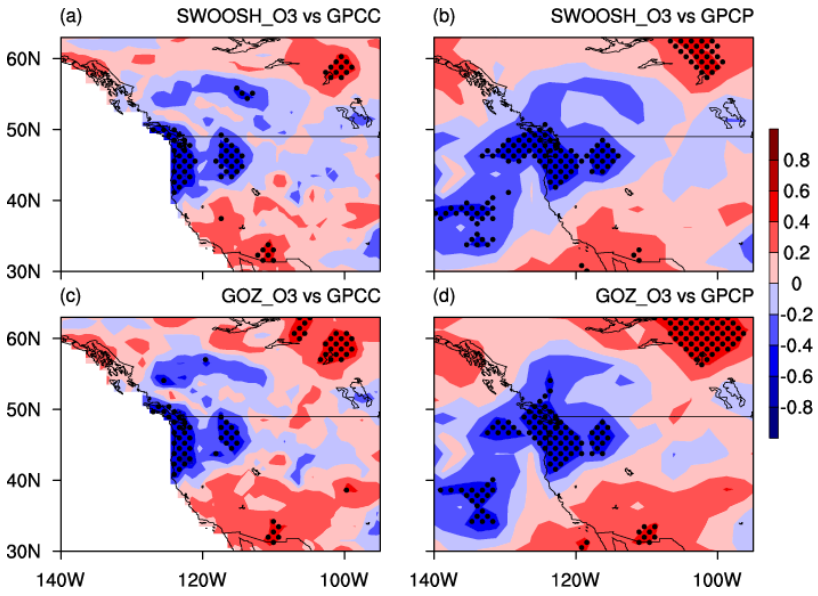

687

688 **Figure 1.** Correlation coefficients between March ASO and April precipitation

689 variations calculated from SWOOSH (a, b) and GOZCARDS (c, d) ozone, and GPCC

690 (a, c) and GPCP (b, d) rainfall for the period 1984–2016. Dots denote significance at

691 the 95% confidence level, according to Student's t-test. The long-term linear trend

692 and seasonal cycle in all variables were removed before the correlation analysis.

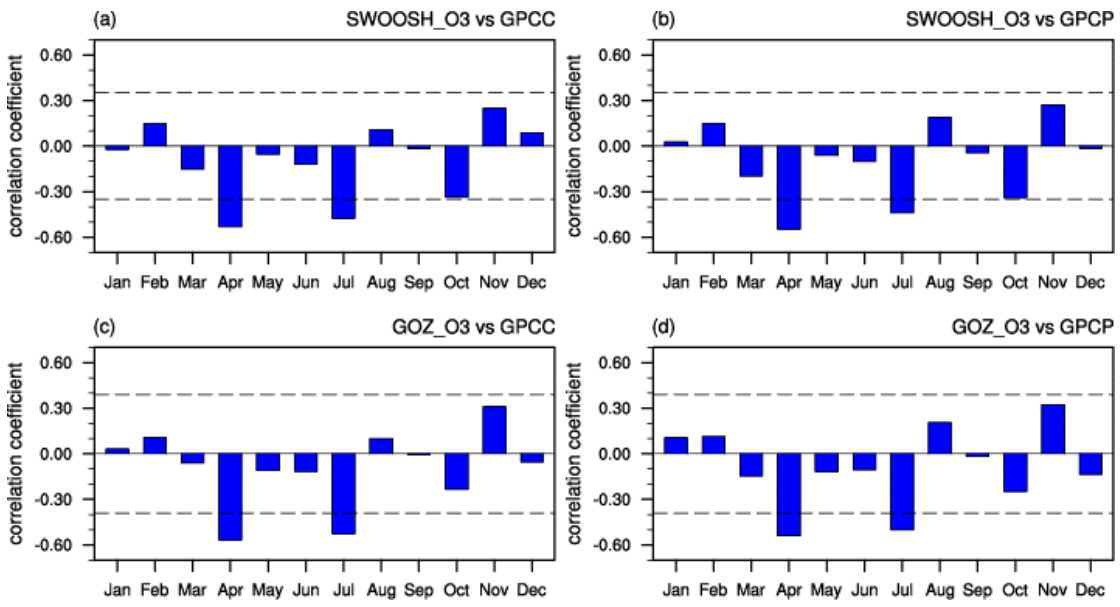

693

694 **Figure 2.** (a) Correlation coefficients between March ASO index and precipitation
695 anomalies in the northwestern US (43°–50°N, 115°–130°W) for each month
696 calculated from SWOOSH (a, b) and GOZCARDS (c, d) ozone, and GPCC (a, c) and
697 GPCP (b, d) rainfall for the period 1984–2016. The dashed blacked lines refer to the
698 correlation coefficient that is significance at 95% confidence level. The long-term
699 linear trend and seasonal cycle were removed from the original datasets before
700 calculating the correlation coefficients.

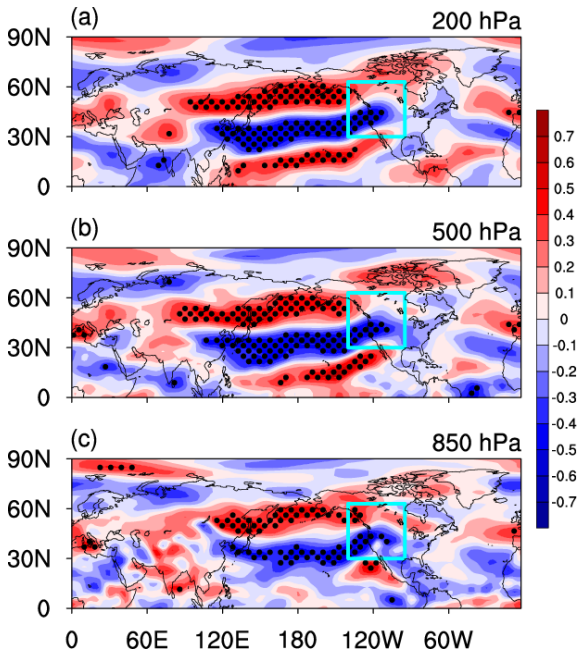

Figure 3. Correlation coefficients between March ASO index and April zonal wind variations (m/s, from NCEP2) from 1984 to 2016 at 200 hPa (a), 500 hPa (b), and 850 hPa (c). Dots denote significance at the 95% confidence level, according to Student's *t*-test. Blue square is the area shown in Fig. 1. Before performing the analysis, the seasonal cycle and linear trend were removed from the original datasets.

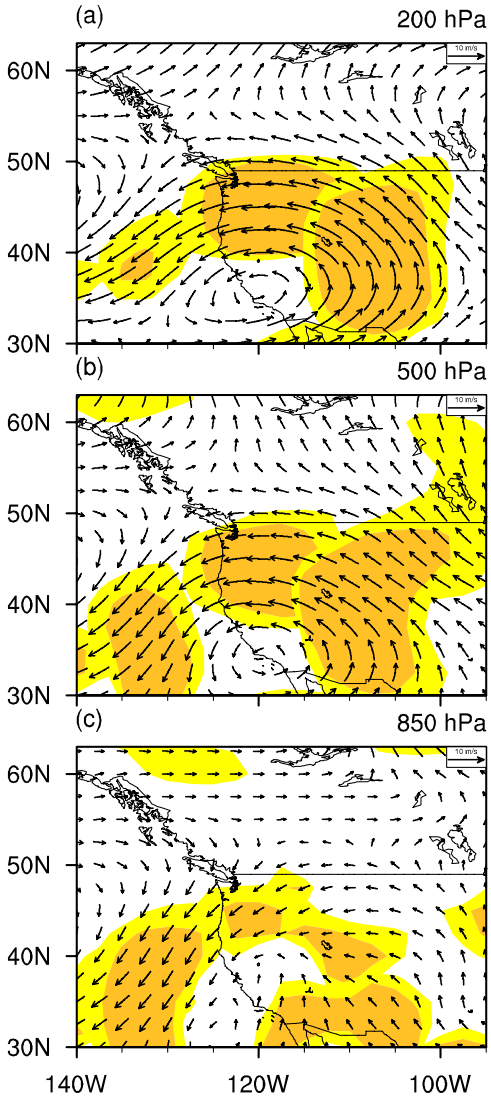

Figure 4. Differences in composite April winds (vectors, m/s, from NCEP2) between positive and negative ASO anomaly events at 200 hPa (a), 500 hPa (b), and 850 hPa (c) for 1984–2016. Colored regions are statistically significant at the 90% (light yellow) and 95% (dark yellow) confidence levels. The seasonal cycle and linear trend were removed from the original dataset. The ASO anomaly events are selected based on Table 2.

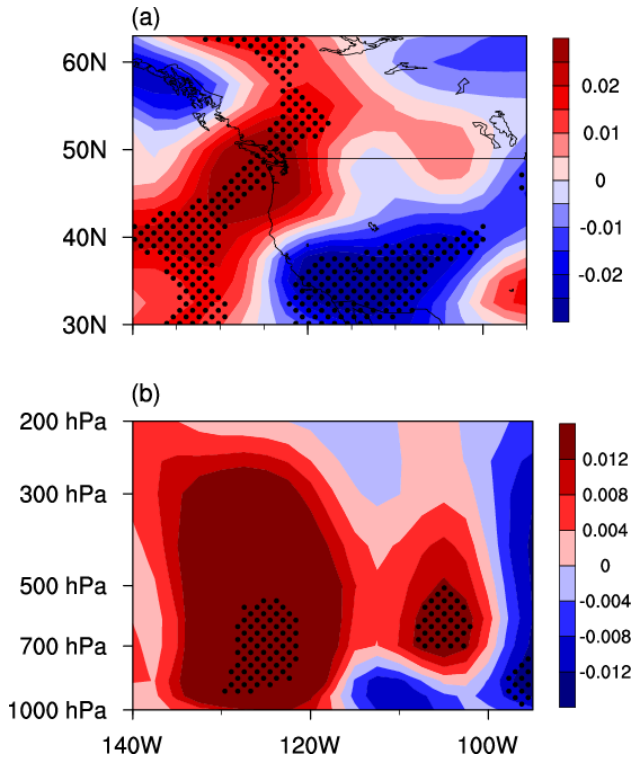

Figure 5. (a) Longitude–latitude cross-section of differences in composite April vertical velocity anomalies (averaged over 1000–500 hPa) between positive and negative ASO anomaly events for 1984–2016. (b) Longitude–height cross-section of differences in composite April vertical velocity anomalies (averaged over 43°–50°N) between positive and negative ASO anomaly events from 1984 to 2016. Blue is upward motion and red is downward motion. Dots denote significance at the 95% confidence level. Before performing the analysis, the seasonal cycle and linear trend were removed from the original dataset. The ASO anomaly events are selected based on Table 2. The vertical velocity (Pa/s) dataset is from NCEP2.

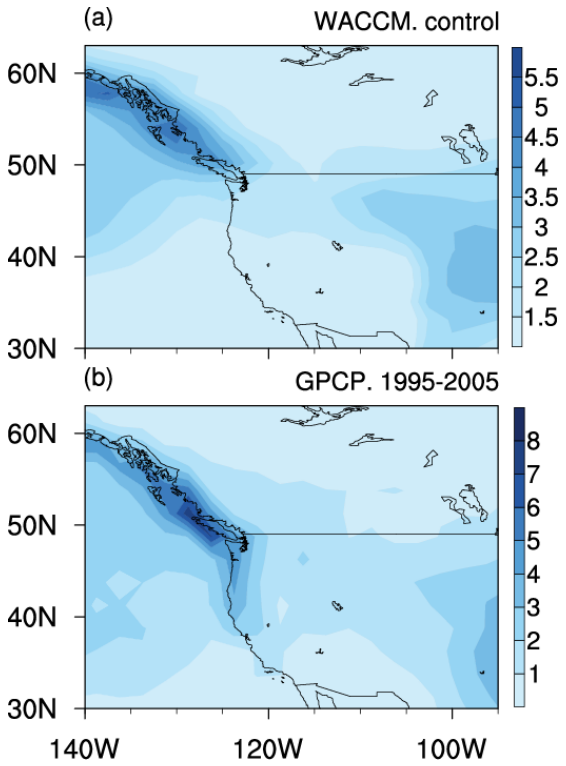

724

725 **Figure 6.** (a) Spatial distribution of April precipitation (mm/day) climatology in the

726 control experiment (R1). (b) Same as (a), but precipitation from the GPCP for the

727 period 1995–2005. For details of specific experiments, see Table 1.

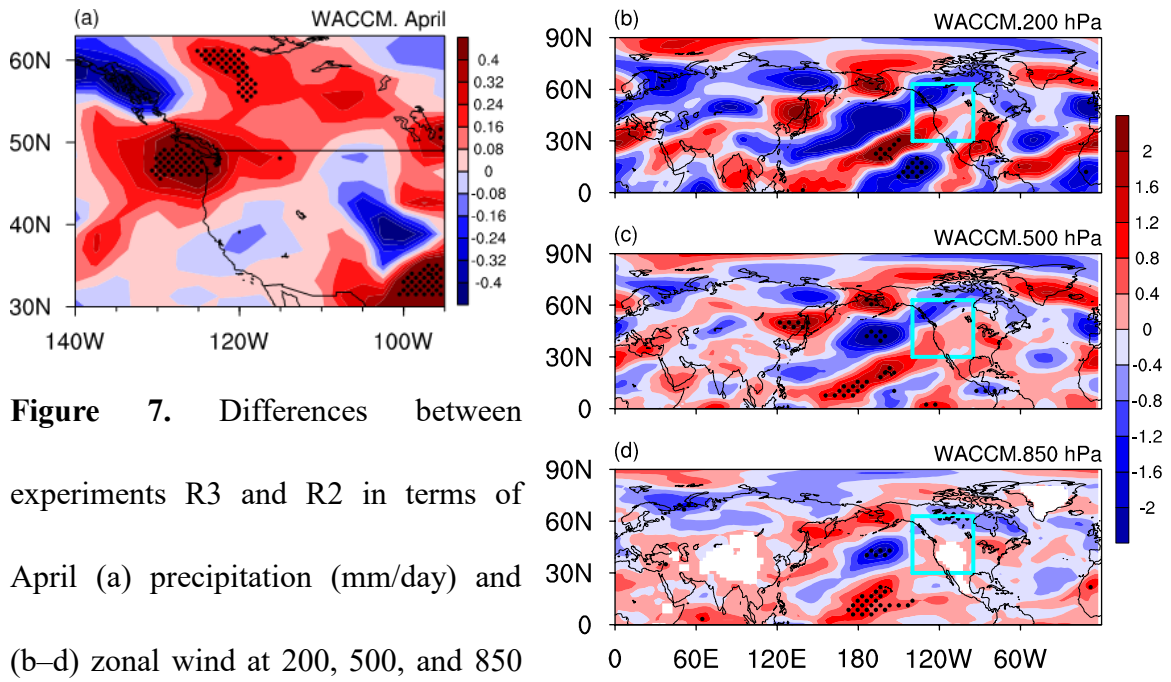

Figure 7. Differences between experiments R3 and R2 in terms of April (a) precipitation (mm/day) and (b–d) zonal wind at 200, 500, and 850 hPa, respectively. Dots denote significance at the 95% confidence level.

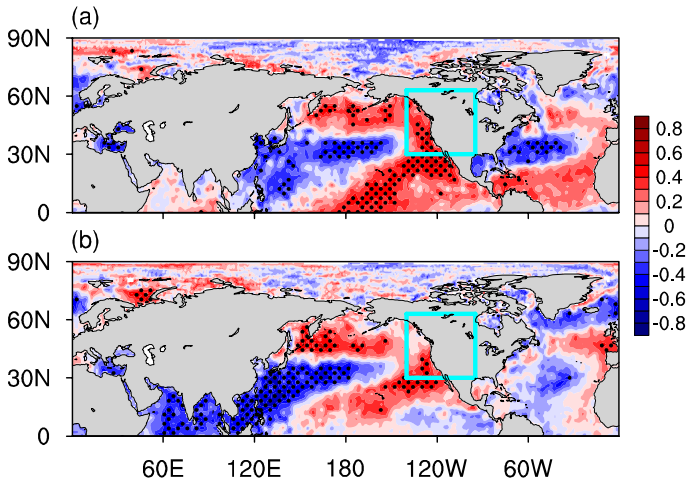

Figure 8. (a) Correlation coefficients between regional precipitation (43°–50°N, 115°–130°W) and SST variations in April for 1984–2016. (b) Correlation coefficients between March ASO (× –1) and April SST variations for 1984–2016. Dots denote significance at the 95% confidence level, according to Student's *t*-test. Before performing the analysis, the seasonal cycle and linear trend were removed from the original data. ASO data are from SWOOSH, precipitation from GPCP, and SST from HadSST.

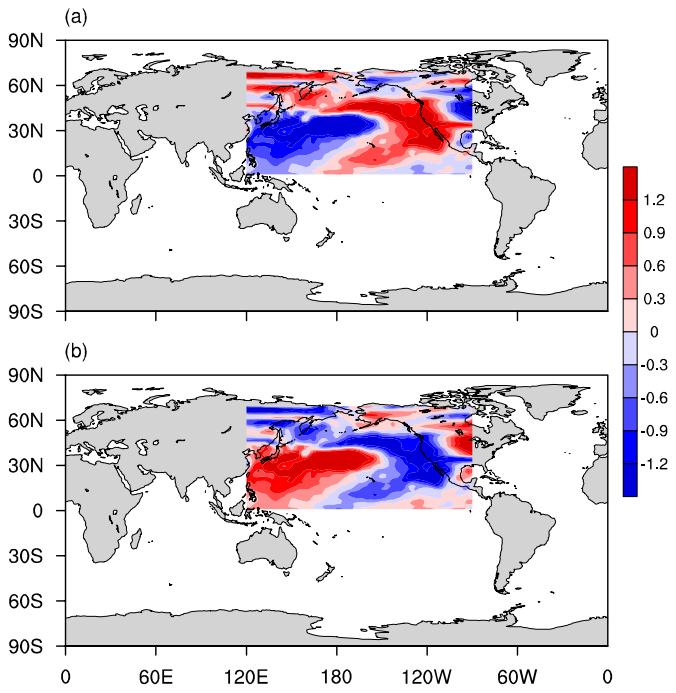

742

743 **Figure 9.** (a) Composite SST anomalies during negative ASO anomaly events. (b)

744 Composite SST anomalies during positive ASO anomaly events. The ASO anomaly

745 events are selected based on Table 2. SST data are from CESM SST forcing data.

746

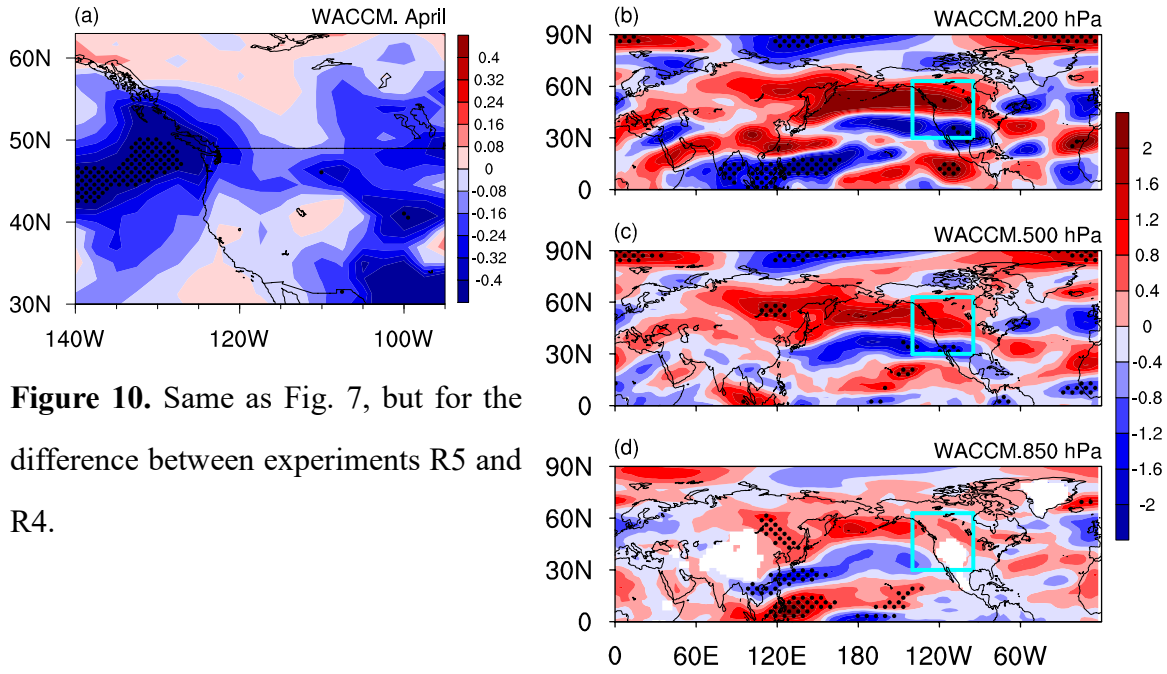

Figure 10. Same as Fig. 7, but for the difference between experiments R5 and R4.

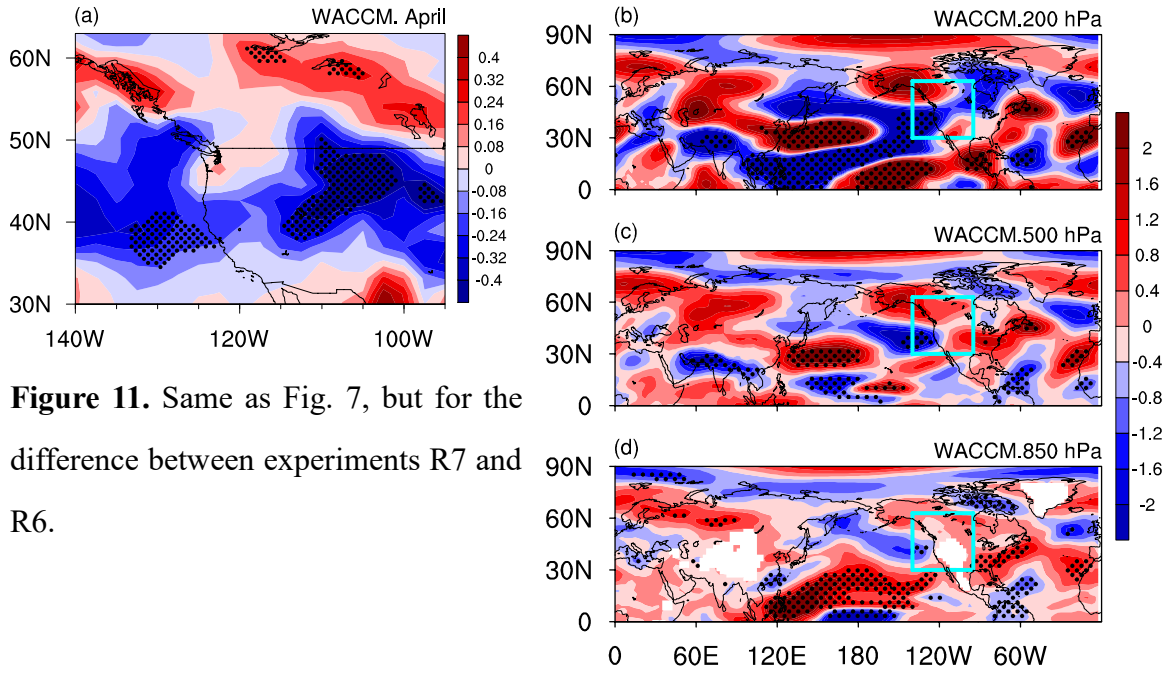

Figure 11. Same as Fig. 7, but for the difference between experiments R7 and R6.

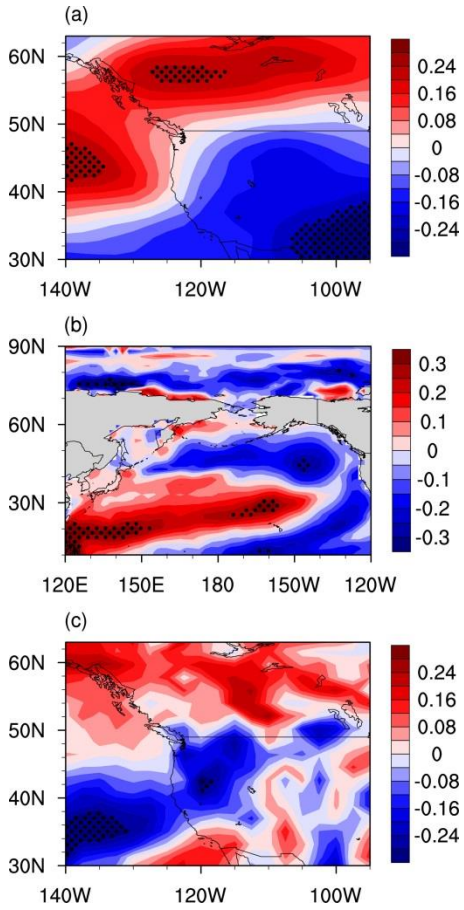

761

762 **Figure 12.** Correlation coefficients between the specified March ASO variations and
763 simulated anomalies of April U (a), SST (b), and precipitation (c) for the period 1955–
764 2005 based on the transient experiment R8. Regions above the 95% confidence level
765 are dotted. The seasonal cycle and linear trend were removed from all quantities
766 before correlation.

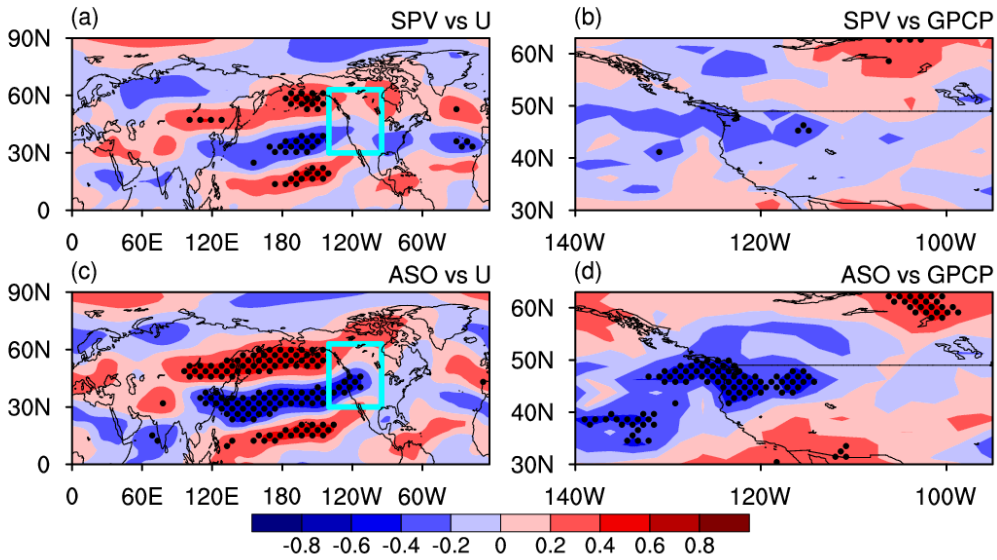

767

768 **Figure 13.** (a) Correlation coefficients between the February –SPV (10^5 K m^2 kg^{-1} s^{-1})
769 index defined by Zhang et al. (2018) and April zonal wind variations at 200 hPa for
770 1984–2016. (b) Correlation coefficients between February –SPV index and April
771 precipitation variations. (c) and (d) As for (a) and (b), but between March ASO and
772 April 200 hPa zonal wind and April precipitation variations. Dots denote significance
773 at the 95% confidence level, according to Student's *t*-test. The long-term linear trend
774 and seasonal cycle in all variables were removed before the correlation analysis. The
775 ASO data are from SWOOSH, zonal wind from NCEP2, and precipitation from
776 GPCP.